INFECTION AND IMMUNITY, Jan. 2006, p. 88–98 Vol. 74, No. 1
0019-9567/06/$08.00+0 doi:10.1128/IAI.74.1.88–98.2006

Dissection of ESAT-6 System 1 of *Mycobacterium tuberculosis* and Impact on Immunogenicity and Virulence

Priscille Brodin,[1] Laleh Majlessi,[2] Laurent Marsollier,[1] Marien I. de Jonge,[1] Daria Bottai,[1] Caroline Demangel,[1] Jason Hinds,[3] Olivier Neyrolles,[4] Philip D. Butcher,[3] Claude Leclerc,[2] Stewart T. Cole,[1] and Roland Brosch[1]*

Unité de Génétique Moléculaire Bactérienne,[1] Unité de Biologie des Régulations Immunitaires–INSERM E352,[2] and Unité de Génétique Mycobactérienne–CNRS URA 2172,[4] Institut Pasteur, 25-28, Rue du Docteur Roux, 75724 Paris Cedex 15, France, and Bacterial Microarray Group, Medical Microbiology, Department of Cellular and Molecular Medicine, St. George's Hospital Medical School, Cranmer Terrace, London SW17 0RE, United Kingdom[3]

Received 8 June 2005/Returned for modification 14 July 2005/Accepted 18 September 2005

The dedicated secretion system ESX-1 of *Mycobacterium tuberculosis* encoded by the extended RD1 region (extRD1) assures export of the ESAT-6 protein and its partner, the 10-kDa culture filtrate protein CFP-10, and is missing from the vaccine strains *M. bovis* BCG and *M. microti*. Here, we systematically investigated the involvement of each individual ESX-1 gene in the secretion of both antigens, specific immunogenicity, and virulence. ESX-1-complemented BCG and *M. microti* strains were more efficiently engulfed by bone-marrow-derived macrophages than controls, and this may account for the enhanced in vivo growth of ESX-1-carrying strains. Inactivation of gene *pe35* (Rv3872) impaired expression of CFP-10 and ESAT-6, suggesting a role in regulation. Genes Rv3868, Rv3869, Rv3870, Rv3871, and Rv3877 encoding an ATP-dependent chaperone and translocon were essential for secretion of ESAT-6 and CFP-10 in contrast to *ppe68* Rv3873 and Rv3876, whose inactivation did not impair secretion of ESAT-6. A strict correlation was found between ESAT-6 export and the generation of ESAT-6 specific T-cell responses in mice. Furthermore, ESAT-6 secretion and specific immunogenicity were almost always correlated with enhanced virulence in the SCID mouse model. Only loss of Rv3865 and part of Rv3866 did not affect ESAT-6 secretion or immunogenicity but led to attenuation. This suggests that Rv3865/66 represent a new virulence factor that is independent from ESAT-6 secretion. The present study has allowed us to identify new aspects of the extRD1 region of *M. tuberculosis* and to explore its role in the pathogenesis of tuberculosis.

Secreted proteins of *Mycobacterium tuberculosis* have long been known to be a rich source of immunogens (39), but for many of them the molecular basis of their export is still poorly understood. It is well established that proteins containing typical signal sequences, such as the highly immunogenic T-cell antigens 85A, 85B, and 85C are secreted by the SecA1 mediated general secretory pathway (33, 44). The analysis of the genome sequence of *M. tuberculosis* H37Rv (13) revealed the presence of a second SecA-like protein, SecA2. This protein was shown to be involved in the secretion of superoxide dismutase SodA, an enzyme that is implicated in the oxidative stress response and lacks a signal sequence (5). In addition, export of some proteins is likely to occur via the twin-arginine translocation (TAT) system, as genes encoding proteins with putative TAT-specific signal sequences were identified in the *M. tuberculosis* genome (10). Small, highly immunogenic proteins that lack classical signal sequences can also be found in mycobacterial culture filtrate. Many of these proteins belong to the 23-membered Esx family (43). Among them, the 6-kDa early secreted antigenic target ESAT-6 (39) and the 10-kDa culture filtrate protein CFP-10 (4) are both encoded by the region of difference 1 (RD1).

* Corresponding author. Mailing address: Unité de Génétique Moléculaire Bactérienne, Institut Pasteur, 25-28, Rue du Docteur Roux, 75724 Paris Cedex 15, France. Phone: (33) 145688449. Fax: (33) 140613583. E-mail: rbrosch@pasteur.fr.

Comparative genomics of the *M. tuberculosis* complex revealed that overlapping portions of RD1 are absent from the attenuated or avirulent strains *Mycobacterium bovis* BCG (BCG) (3, 22, 28), *Mycobacterium microti* (7), and the Dassie bacillus (31) but are present in all fully virulent isolates (12). Complementation of BCG and *M. microti* with RD1, using integrating cosmid pRD1-2F9, resulted in increased virulence in mice (8, 34) (29), and deletion of RD1 from *M. tuberculosis* leads to attenuation of the strain (24, 27). Genetic approaches coupled to biochemical analyses showed that proteins encoded by the RD1 locus are part of a secretion system required for both ESAT-6 and CFP-10 export (9, 23, 24, 35, 40), hereafter named ESAT-6 system-1 (ESX-1) (9). However, details of the elements constituting the ESX-1 secretion system, as well as the mechanisms by which ESX-1 may affect the host-pathogen interaction, remain largely unknown. Therefore, in the present study, BCG and/or *M. microti* strains, and their RD1 complemented counterparts, were subjected to comparative analyses, by determining two-dimensional protein patterns; in vitro, ex vivo, and in vivo growth characteristics; and transcriptional profiles. Systematic inactivation or deletion of genes on cosmid pRD1-2F9 and analysis of these constructs in recombinant BCG and/or *M. microti* allowed us to determine which genes were required for ESAT-6 and CFP-10 secretion in addition to those previously identified. Moreover, these constructs were used to investigate the influence of ESX-1 and each of its different components on RD1-mediated, antigen-specific immunogenicity and virulence.

MATERIALS AND METHODS

Genetic constructs and mycobacterial strains. Inactivation of genes in cosmid pRD1-2F9, previously used for the expression and secretion of ESAT-6 by BCG and *M. microti* OV254 was accomplished by two approaches. First, pRD1-2F9 was digested with endonucleases SnaBI, AvrII, HpaI, or XbaI that had only one or two restriction sites in the plasmid. Apramycin cassettes were PCR amplified with oligonucleotides that contained these restriction sites at the 5′ ends, using pUC-derived plasmids as templates. After digestion and purification, apramycin cassettes were individually ligated into pRD1-2F9 and then electroporated into DH10B cells (Invitrogen, Carlsbad, CA), generating constructs that had Rv3870 (SnaBI), Rv3871 (AvrII), *ppe68* (HpaI), or Rv3876 (XbaI) inactivated by insertion of a cassette. In addition, AscI was used to excise a fragment spanning from the 3′ end of Rv3868 to the middle of Rv3869, while PmlI was used to excise from pRD1-2F9 a fragment spanning Rv3878 to Rv3881. Genes for which suitable restriction sites were not available were inactivated by transposon insertion using the EZ::TN kan2 in vitro transposition kit (Epicenter, Madison, WI) according to the manufacturer's instructions. By this approach, knockout (ko) constructs were obtained for Rv3864, Rv3867, Rv3868, Rv3869, *pe35*, and Rv3877. The EZ::TN kan2 transposon contains a restriction site for Sse8387, which is also present in the vector backbone of pRD1-2F9 just upstream of *rv3860*. In selected clones, digestion with Sse8387, gel purification, and religation allowed us to remove fragments, which were situated between the Sse8387 site upstream of Rv3860 and the insertion site of the transposon. Constructs ΔRv3860-64 and ΔRv3860-66 were obtained by this strategy. Finally, to delete selected fragments from the flanking regions of genes *esxB* and *esxA*, a 1.5-kb HpaI/SapI fragment was subcloned into modified pUC19 (NEB) and subjected to genetic modification by using two pairs of oligonucleotides containing selected restriction sites. Modified 1.5-kb fragments were cloned into HpaI/SapI-cut pRD1-2F9 from which the original 1.5-kb fragment had been removed. By this approach, partial or complete CFP-10 or ESAT-6 in-frame deletion mutants were constructed (Δ*esxB*, Δ*esxA*, *esxA*Δ*3-24*, *esxA*Δ*76-95*, and *esxA*Δ*84-95*). Modification of the 1.5-kb fragment was also used for the Δprom(*esxB/A*) and Δ*ppe68* constructs, deleting fragments spanning from positions 4352123 to 4352235 and from positions 4351558 to 4352100, respectively. A similar method was used for constructs ΔRv3876, in which the SapI-XbaI fragment in *rv3876* was replaced by a small PCR product containing compatible ends. To clone large RD1 fragments from *M. tuberculosis*, we used the single NheI restriction site of vector pYUB412 (2) to insert NheI-digested fragments according to a previously described cloning procedure (11). This approach generated construct pNheI-Rv3869-79, containing an NheI fragment of *M. tuberculosis* H37Rv that spans region from positions 4343610 to 4360040. XhoI restriction profiles of all of the different constructs were generated and compared to the original pRD1-2F9 profile for control purposes, and undigested high concentrated plasmid DNA preparations were then electroporated into electrocompetent cells of *M. tuberculosis* H37RvΔRD1 (a gift from William R. Jacobs, Jr.) (24), BCG, or *M. microti* OV254 as previously described (8, 34) by using a Bio-Rad Gene Pulser (Bio-Rad, Munich, Germany). Hygromycin-resistant colonies appearing after 3 to 4 weeks were analyzed for the presence of the integrated vector by PCR using primers specific for RD1-encoded genes as previously described (7).

RNA extraction, cDNA labeling, and microarray experiments. RNA were extracted from 50 ml of an exponential-phase broth culture at day 15 after inoculation with a preculture according to the procedure previously described (42). RNA quality and quantity were assessed on an Agilent 2100 bioanalyzer by using the RNA 6000 Nano LabChip Kit. cDNA was labeled by incorporation of Cy3 or Cy5 dCTP during reverse transcription of RNA (Amersham, Uppsala, Sweden) and hybridized on whole-genome microarrays supplied by the Bacterial Microarray Group at St. Georges's (BμG@S [http://www.bugs.sghms.ac.uk]). Independent sets of data from two RNA samples batches followed by dye swap labeling were analyzed using GeneSpring software (Silicon Genetics, Redwood City, CA) as recommended by BμG@S. Fully annotated microarray data has been deposited in BμG@Sbase (accession number E-BUGS-31 [http://bugs.sgul.ac.uk/E-BUGS-31]) and also ArrayExpress (accession number E-BUGS-31). Radiolabeled cDNA from the *M. tuberculosis* H37RvΔRD1::RD1-2F9-pe35 ko mutant for macroarray experiments was obtained by incorporation of [^{32}P]dCTP during reverse transcription of RNA. Spotting and hybridization of the arrays was done as previously described (30).

Macrophage internalization assays. Bone-marrow-derived macrophages were obtained by seeding 5×10^4cells bone marrow cells from 8-week-old C57BL/6 mice per well in Dulbecco modified Eagle medium with low glucose (1 g/liter) and high carbonate (3.7 g/liter) concentrations, supplemented with 10% heat-inactivated fetal calf serum, 10% L-cell-conditioned medium, and 2 mM L-glutamine. Culture medium was changed at day 4 and then every 3 days, with cells being differentiated after 7 days. Activated macrophages were prepared by incubation with 100 U of gamma interferon (IFN-γ) and 10 ng of lipopolysaccharide (LPS) (Sigma, Saint Louis, MO)/ml 24 h prior to infection. Alveolar epithelial A549 cells (American Type Culture Collection) were cultured in RPMI 1640 supplemented with 10% heat-inactivated fetal calf serum. For internalization assays, cells were infected with bacterial suspensions at a multiplicity of infection of 1:1. After 16 h, cells were washed three times with phosphate-buffered saline before the addition of fresh culture medium. For the kinetics study, the number of intracellular bacteria was determined at 4 h, days 3 and 6 after infection by the addition of 0.1% Triton X-100 (Fluka, Buchs, Germany) and serial fold dilutions of cell lysates on Middlebrook 7H11 medium (BD, Sparks, MD) supplemented with oleic acid-albumin-dextrose-catalase (OADC).

Biochemical analysis. *M. bovis* BCG and *M. microti* OV254 recombinants were grown in 20 ml of Sauton liquid medium and 0.05% Tween 80 at 37°C for 6 and 14 days, respectively. Cultures were harvested by centrifugation. The culture filtrate was recovered after filtration through 0.22-μm-pore-size filters (Millex^R GP; Millipore, Bedford, MA), followed by concentration using a filter with a 3-kDa cutoff (Centricon; Millipore). The mycobacterial pellet was washed twice and suspended in Tris 20 mM (pH 7.5) containing protease inhibitors (Complete EDTA Free; Roche Diagnostics GmbH, Mannheim, Germany). Cells were broken by shaking with 106-μm acid washed-glass beads (Sigma, St. Louis, MO) for 8 min at speed 30 in a Mill Mixer (MM300; Retsch GmbH, Haan, Germany). The whole-cell lysate consisted of the supernatant fraction recovered after removal of the debris and centrifugation at 14,000 rpm for 30 min. Alternatively, for further fractionation, beads and unbroken cells were firstly discarded by a 30-min centrifugation at 5,000 rpm. The resulting supernatant was then subjected to a 45-min centrifugation at 14,000 rpm. The cell wall fraction consisted of the pellet, and the supernatant was further centrifuged at 65,000 rpm for 90 min on a TL-100 ultracentrifuge (Beckman, Fullerton, CA). The cytosolic and membrane fractions correspond to the resulting supernatant and pellet, respectively. Total protein concentrations were determined by using a Bio-Rad protein assay (Bio-Rad), and 20-μg samples were subjected to sodium dodecyl sulfate-polyacrylamide gel electrophoresis (SDS-PAGE). Immunoblot analysis were carried out with mouse ESAT-6 monoclonal antibody (Hyb 76-8; Statens Serum Institute, Copenhagen, Denmark) and His-tag H-15 (Santa Cruz Biotechnology, Santa Cruz, CA), CFP-10, and PPE68 rabbit polyclonal antibodies.

Virulence studies and immunological analyses. Mycobacterial strains were grown and suspensions prepared as described previously (8). Six-week-old male C.B-17/Icr Ico SCID mice, female C57BL/6 mice (Charles River, St. Germain sur l'Arbresle, France), tumor necrosis factor alpha (TNF-α) ko mice (B6;129-LT-α/TNF-α tm1; CDTA, Orléans, France), IFN-γ receptor ko mice (inbred 129/Sv mice obtained from Michel Aguet [25] by Jean-François Bureau [Institut Pasteur, Paris, France] and bred at Pasteur Institute Facility since 1993) were infected intravenously (10^6 CFU). Organs from sacrificed mice were homogenized by using an MM300 (QIAGEN, Hilden, Germany) apparatus and 2.5-mm-diameter glass beads. Serial fivefold dilutions in medium were plated on 7H11 agar with 50 μg of hygromycin ml^{-1} when appropriate, and the CFU count was ascertained after 4 weeks of growth at 37°C for *M. microti* recombinant strains and 3 weeks for recombinant BCG.

For immunological studies, adult C57BL/6 (*H-2^b*) mice were injected subcutaneously with 10^6 CFU of recombinant *M. microti* and BCG recombinant strains. At 3 weeks postimmunization, splenocytes were cultured (10^6 cells/well), and IFN-γ production was assessed with 10 μg of purified protein derivatives (Statens Serum Institute)/ml; 4 μg of recombinant ESAT-6, CFP-10, or MalE/ml; or 10 μg of synthetic peptides (kindly provided by Marcella Simsova and Peter Sebo)/ml. After 72 h of incubation, amounts of IFN-γ were quantified in culture supernatants with a detection limit of 500 pg/ml as described elsewhere (29).

RESULTS

Expression of RD1 in vitro triggers secretion of proteins ESAT-6 and CFP-10 but does not affect the bacterial growth rate and gene transcription. In order to determine the possible role of ESX-1 proteins on the bacterial phenotype, we studied the growth rate of RD1-complemented strains in different media and compared their transcriptional and two-dimensional protein profiles to those of parental strains. BCG::RD1 refers to the recombinant BCG strain with pRD1-2F9, spanning Rv3860 to Rv3884 integrated at *attB*, whereas BCG::pYUB412 is the control strain harboring the empty cosmid. Monitoring

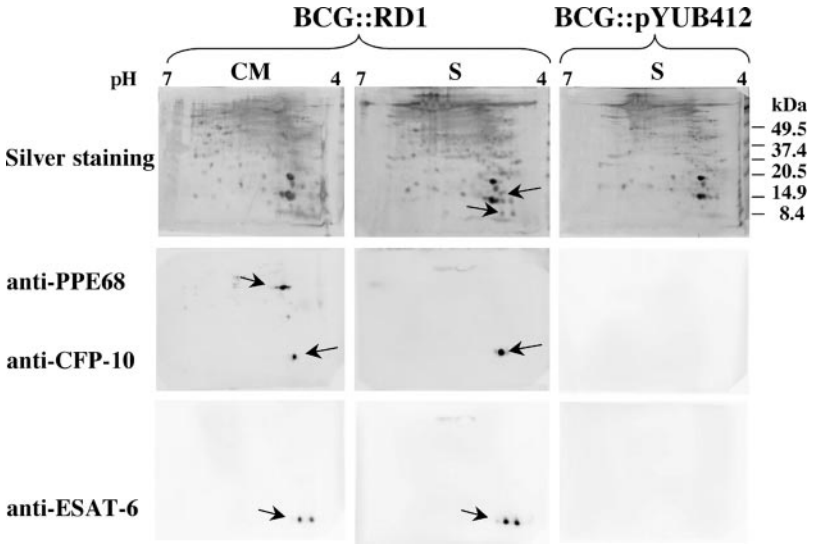

FIG. 1. Two-dimensional analysis of whole-cell extracts (CM) and supernatants (S) of BCG::RD1 and control BCG::pYUB412. Detection was carried out by silver staining (top) and with monoclonal anti-ESAT-6 and polyclonal anti-CFP-10 and anti-PPE68 antibodies for Western blot analysis.

the in vitro growth rate of BCG::RD1 and *M. microti* RD1 showed only minor, statistically insignificant differences relative to vector control strains (data not shown). We then carried out a comparative transcriptome analysis. After differential labeling, RNAs extracted during exponential growth were hybridized to an *M. tuberculosis* H37Rv whole-genome microarray (42). A ratio of 1.5 or higher between the signal of BCG::RD1 relative to the signal of BCG::pYUB412 was obtained for all of the genes located on the inserted pRD1-2F9 cosmid, confirming that the integrated genes from the RD1 region were efficiently expressed by the recombinant BCG strain. Neither upregulation nor downregulation of genes corresponding to Rv2462c and Rv2463 adjacent to the *attB* integration site was noticed. In addition, the expression profiles of other genes outside the RD1 region were not substantially altered, suggesting that the RD1 region does not encode regulators that affect genes elsewhere. Fully annotated microarray data are available via the BμG@Sbase (see Materials and Methods).

In parallel, whole-cell extracts and culture filtrate proteins from exponentially growing BCG::RD1 cultures were analyzed by two-dimensional gel electrophoresis. ESAT-6 and CFP-10 were present in both fractions, whereas the PPE68 protein was only found in whole-cell extract of BCG::RD1 as observed previously (Fig. 1) (16). The amount of secreted ESAT-6 was found to be ca. 10 ng/10^8 bacteria, which corresponds to 0.1% (wt/wt) of total culture filtrate proteins and is ~10-fold greater than the intracellular form. Western blot analysis with antibodies specific for RD1 antigens revealed that ESAT-6 was present in isoforms, visible as two spots that differed in their pI (Fig. 1). The same profiles were obtained for *M. microti*::RD1 relative to *M. microti* controls (data not shown). This suggests that RD1-complemented *M. microti* and BCG indeed represent biologically relevant models for studying ESX-1, since two major spots containing six isoforms of ESAT-6 were also found for wild-type *M. tuberculosis* using the same focusing range from pH 4 to 7 (32). Taken together, our data clearly show that upon integration of the RD1 region, the ESX-1 antigens are constitutively expressed and secreted at a high level without any host selective pressure.

Presence of ESX-1 induced increased uptake of recombinant BCG and *M. microti* in macrophages. Macrophages are important sites of growth and dissemination of intracellular pathogens. Since they represent crucial mediators of innate immunity, macrophages have been used extensively to analyze the host-*Mycobacterium* interactions. To search for the biological role of ESX-1 encoded antigens, we examined whether BCG::RD1 and *M. microti*::RD1 differed from controls in their capacity to enter and proliferate within host cells, as recently suggested by a genome-wide screen of transposon mutants (36). Murine bone-marrow-derived macrophages were infected overnight with exponentially growing bacteria, and then the number of CFU in lysed cells was determined. Figure 2A shows that BCG::RD1 and *M. microti*::RD1 were engulfed more efficiently than controls. A similar differential effect was also observed with bacteria cultured in the presence of Tween 80, which is commonly used to avoid clumping in broth, thus ruling out the possibility that the higher number of ESX-1-expressing bacteria inside macrophages is due to the uptake of bacterial aggregates. The same trend of increased uptake was noted for *M. tuberculosis* H37Rv relative to *M. tuberculosis* H37Rv-ΔRD1 after 4 h of infection (data not shown). Moreover, such differential uptake was not observed with human A549 epithelial cell-like cells (data not shown), suggesting that increased internalization of the RD1-expressing strain was restricted to professional phagocytic cells. Although *M. tuberculosis* was able to multiply in host macrophages, no growth was observed for the BCG vector control and BCG::RD1 (Fig. 2B). In addition, in LPS- and IFN-γ-activated macrophages the growth of recombinant and control strains was comparably reduced, whereas *M. tuberculosis* persisted (Fig. 2C). Altogether, these results suggest that ESX-1 proteins may play an

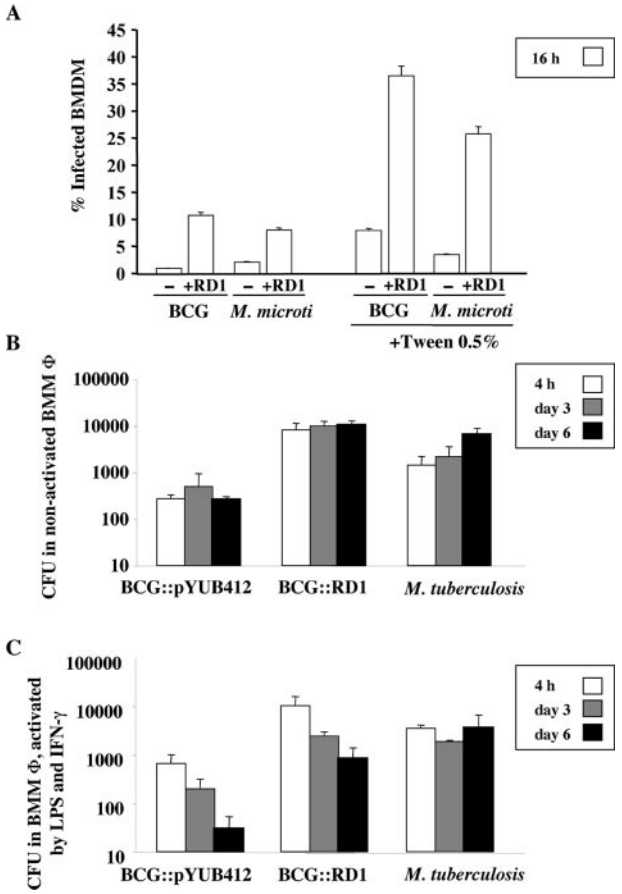

FIG. 2. (A) Quantification of bacterial uptake (%) at 16 h postinfection of murine bone marrow macrophages (BMMΦ) with BCG and *M. microti* expressing the whole RD1 region (+RD1) or not (−) in the presence or absence of Tween 80. CFU in BMMΦ (B) or after activation with LPS and IFN-γ (C) at 4 h (□) and days 3 (▨) and 6 (■) after infection with BCG::pYUB412, BCG::RD1, and *M. tuberculosis* H37Rv. Means and standard deviations are from infections done in quadruplicate wells and are representative of four experiments.

important role for enhanced phagocytosis of ESX-1 containing tubercle bacilli. This hypothesis is in good agreement with recently published results of Renshaw et al., who showed that the ESAT-6–CFP-10 complex specifically binds to the surface of macrophages (37).

Effect of ESX-1 on interaction of bacteria with the host immune system. To further investigate the interaction of ESX-1 with the immune system, the influence of RD1-encoded proteins on bacterial proliferation was evaluated in different mouse models. We have previously reported that in severe combined immunodeficient (SCID) mice, the virulence of BCG increases upon integration of the ESX-1 system, showing 2- to 3-log-higher bacterial loads in spleens and lungs (34), with mean survival times of BCG::RD1-infected animals nearing those infected with *M. tuberculosis* (8). The same trend was observed in the present infection study for SCID mice having received BCG::RD1 or BCG::pYUB412 (Fig. 3A and B). However, in immunocompetent mice (e.g., C57BL/6), intravenous infection with BCG::RD1 did not induce such marked effects, i.e., differential growth was minor in the spleen but stronger in the lungs compared to the

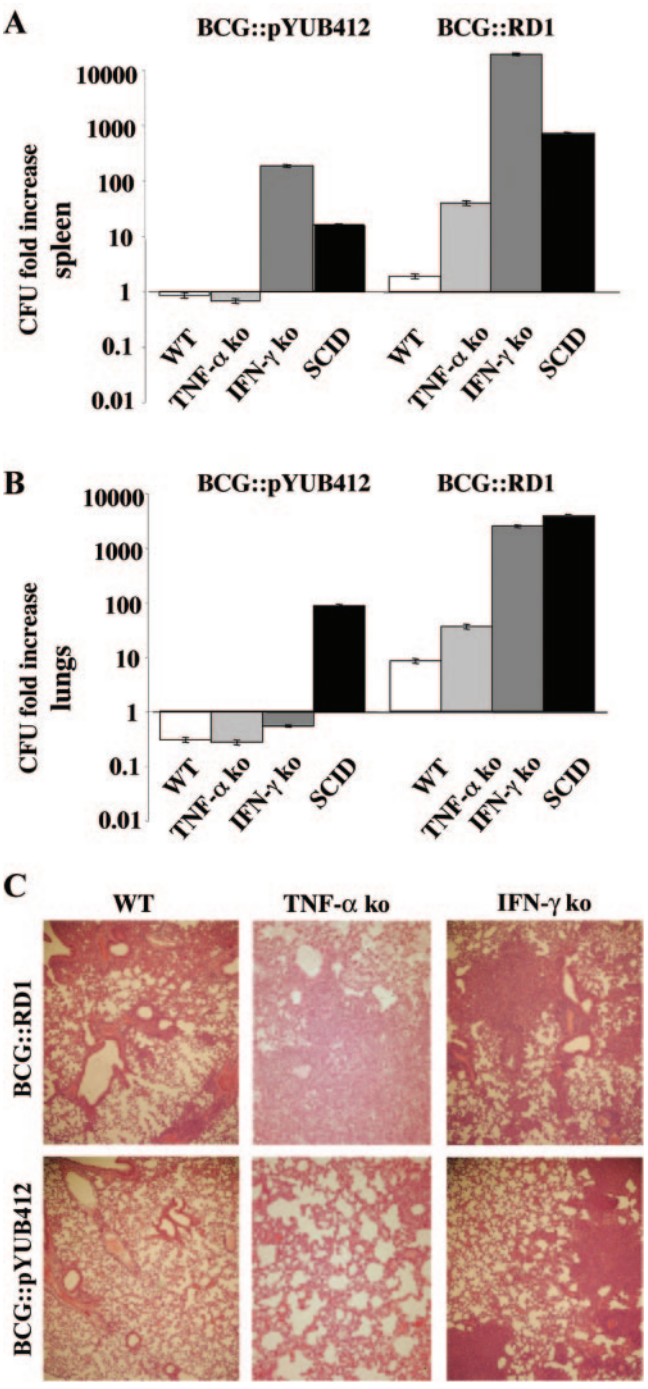

FIG. 3. In vivo bacterial replication of BCG::RD1 in various mouse models: C57BL/6 wild-type mice (open bars), B6;129-LT-α/TNF-α ko mice (light gray bars), inbred 129/Sv IFN-γ receptor ko mice (dark gray bars), and SCID mice (black bars). The ratios of CFU counts at day 28 in spleen (A) and lungs (B) relative to initial dose after intravenous infection with 10^6 CFU are indicated. Each value is the mean of three or four mice, and the error bars represent standard deviations. (C) Histological samples of lungs from C57BL/6 wild type (WT), TNF-α ko, and IFN-γ receptor ko mice, showing compact discrete lesions in lungs of C57BL/6 mice and large diffuse lesions for TNF-α ko mice infected with BCG::RD1 compared to the absence of lesions in wild-type and TNF-α ko mice infected with the BCG vector control. Lungs from IFN-γ receptor ko mice showed lesions with both strains, although bacterial counts were lower for the vector control. Sections were stained with hematoxylin and eosin. Magnification, ×100.

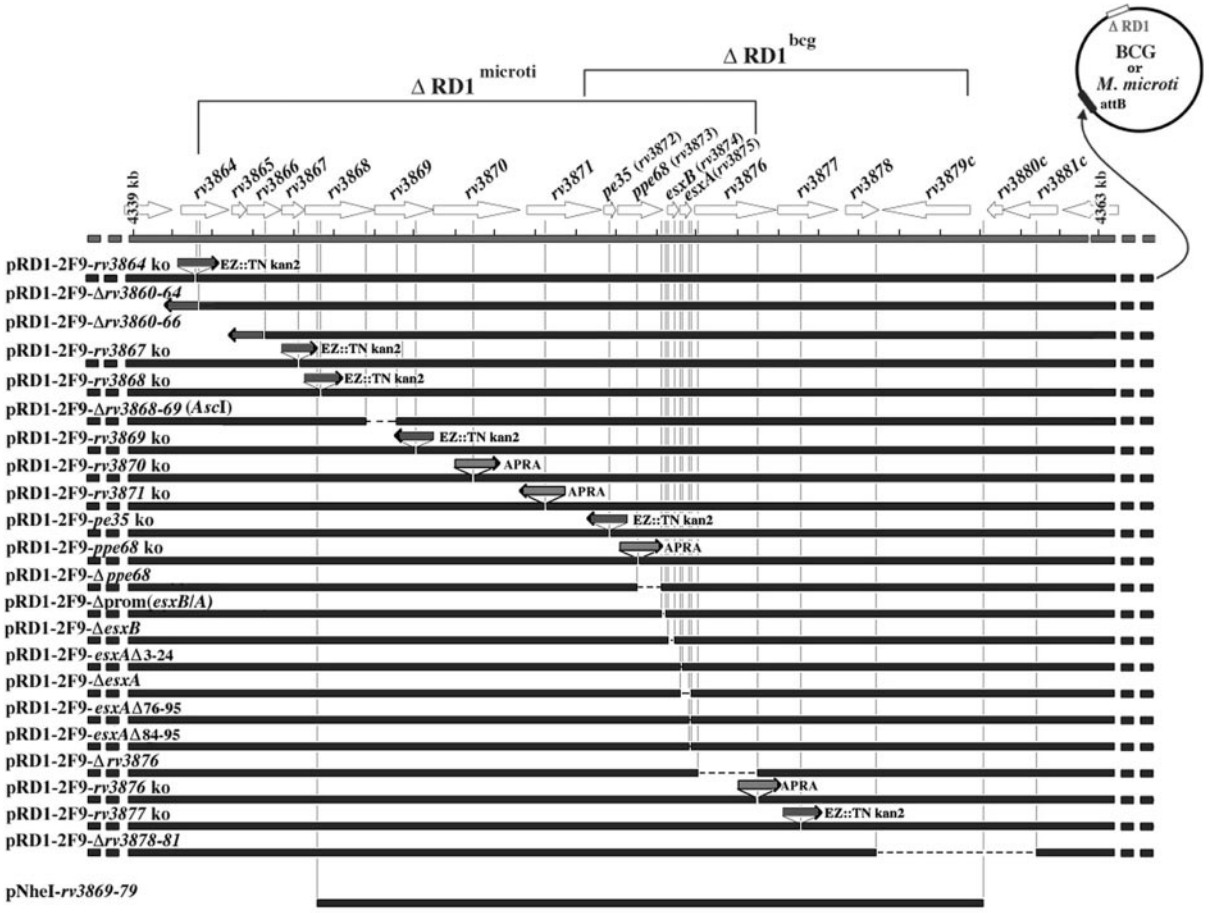

FIG. 4. Scheme of the various pRD1-2F9 and pNheI constructs that were integrated into BCG and *M. microti*. Within the genome shown as a circle, ΔRD1 refers to the naturally occurring RD1 deletions in *M. microti* and BCG. For each construct (the name is given above on the left), the site of the transposon insertion (EZ::TN kan2), apramycin cassette (APRA), or deletion (—) in the corresponding open reading frames relative to its position in RD1 region is shown. The orientation of the transposon/cassette is shown by the direction of the arrow. *pe35*, *ppe68*, *esxB*, and *esxA* correspond to Rv3872, Rv3873, Rv3874, and Rv3875.

control (Fig. 3A and B), suggesting that infection with RD1-expressing strains can be efficiently controlled by the host immune system. To better understand the role of the immune system in the control of bacterial growth in vivo, the effect of ESX-1 on virulence was further investigated in mice lacking TNF-α or impaired in IFN-γ signaling, two key cytokines involved in response to mycobacterial infection (18, 19, 25). Whereas BCG growth was not significantly modified by absence of TNF-α expression, BCG::RD1 replicated significantly better in TNF-α-deficient animals than in wild-type controls (Fig. 3A and B) and induced extensive lesions in lungs (Fig. 3C). Proliferation of BCG::RD1 was even more enhanced in IFN-γ receptor-deficient mice, with CFU numbers 1,000 times higher than those observed in wild-type controls. Lungs from these mice showed lesions with both strains, although fewer bacteria were detected for the BCG vector control (data not shown). These results suggest that immune responses induced by ESX-1 antigens are generated at both the innate and adaptive levels to limit mycobacterial replication of RD1-complemented strains. This finding led us to search for the key players involved in these processes.

Genes Rv3868 to *pe35* but not Rv3864 to Rv3867 are required for expression and secretion of ESAT-6 and CFP-10. In order to identify the ESX-1 genes involved in the phenotypic changes, we constructed a series of modified cosmids, wherein each gene was inactivated either by insertion of an antibiotic cassette, by in vitro transposon mutagenesis, or by small deletions from pRD1-2F9 or pNheI vectors (Fig. 4). These cosmids were subsequently used to complement *M. microti* OV254, BCG, or *M. tuberculosis* H37RvΔRD1 (24), a strain which lacks the same RD1 region as BCG. Due to differences in the size of the RD1 deletion, *M. microti* naturally lacks Rv3864 to Rv3876 and BCG lacks Rv3871 to Rv3879 (Fig. 4). *M. microti* was therefore used as host strain to evaluate the effects of inactivation of *rv3864* to *rv3870*, whereas the effects of interruption of Rv3871 to Rv3879 were tested in BCG and/or *M. tuberculosis* H37RvΔRD1. Some constructs were tested in several strains. The recombinant strains were first screened for their ability to produce and secrete ESAT-6 and CFP-10 proteins as monitored by the presence of these antigens in different fractions. The absence of PPE68 from culture filtrate was used as an internal control for absence of cell lysis.

M. microti strains containing variants of pRD1-2F9, lacking either Rv3860 to Rv3864 or Rv3860 to Rv3866, clearly secreted ESAT-6 and CFP-10 (ΔRv3860-66 [Fig. 5A]). In ad-

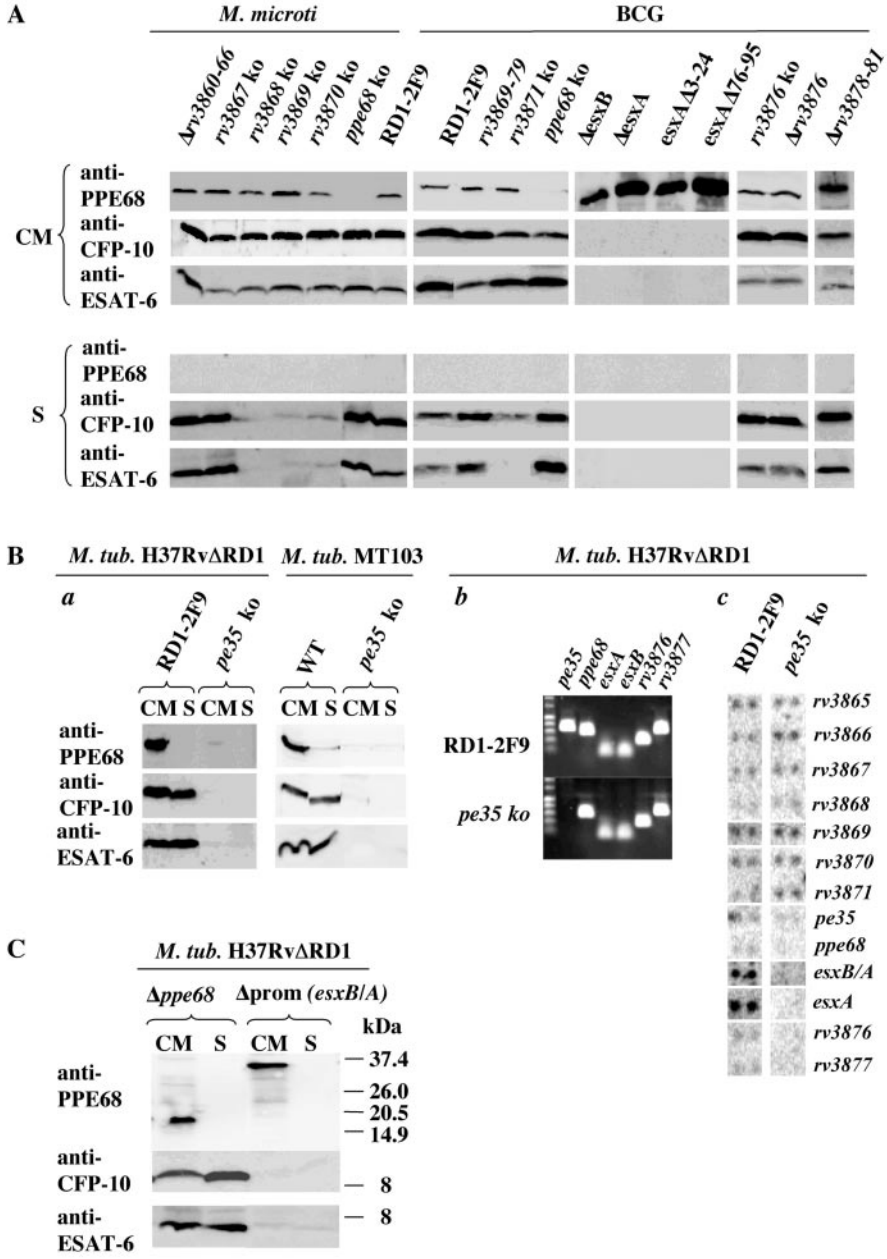

FIG. 5. Secretion analysis. In vitro expression and secretion of ESX-1 antigens from recombinant *M. microti*, BCG, and *M. tuberculosis* H37RvΔRD1 complemented with integrating cosmids that were mutated in selected RD1 genes was examined. Total protein concentrations were determined by using Bio-Rad protein assay, and 20-μg samples were subjected to SDS-PAGE. PPE68, CFP-10, and ESAT-6 correspond to products encoded by *ppe68* (Rv3873), *esxB* (Rv3874), and *esxA* (Rv3875) genes, respectively. (A) CM, whole-cell extract containing cytosolic and membrane fractions; S, supernatant. Detection was carried out by using monoclonal anti-ESAT-6, polyclonal anti-CFP-10, and polyclonal anti-PPE68 antibodies. (B) Analysis of recombinant *M. tuberculosis pe35* ko and control strains: (a) secretion analysis with same antibodies as described for panel A; (b) PCR control amplification obtained with primers for genes *pe35* to Rv3877 for *pe35* ko and RD1-2F9 *M. tuberculosis* H37RvΔRD1 strains; (c) hybridization signals obtained with radiolabeled cDNA from *M. tuberculosis* H37RvΔRD1::RD1-2F9 and *pe35* ko mutant using a focused mini-array containing PCR products from selected genes of the RD1 region spotted on nylon membranes in duplicates. (C) Secretion analysis of recombinant *M. tuberculosis* strains lacking part of the *ppe68* (Rv3873) gene or the described promoter region of *esxB/A* (*rv3874-75*) (4), with the same antibodies as described for panel A.

dition, ESAT-6 and CFP-10 export by recombinant *M. microti* also occurred from transposon mutant Rv3864 ko or Rv3867 ko strains, suggesting that Rv3864, Rv3865, Rv3866, and Rv3867 are not directly involved in the translocation of ESAT-6 and CFP-10 (Fig. 5A). In contrast, interruption of Rv3868, Rv3869, Rv3870, or Rv3871 resulted in the loss of ESAT-6 and CFP-10 secretion despite normal expression of these antigens. These results were further confirmed by *M. microti*::RD1-2F9ΔRv3868-69 (AscI), and *M. microti*::NheI-Rv3869-79 (Fig. 4), both lacking complete Rv3868 and/or Rv3869 genes. Like

the Rv3868 ko, and Rv3869 ko strains, these strains expressed ESAT-6 and CFP-10 but were unable to secrete the two antigens into the culture supernatant (data not shown). These results indicate that Rv3868 and Rv3869, in addition to the previously identified Rv3870 and Rv3871 (23, 35, 40), are indeed important for efficient export of ESAT-6 and CFP-10.

When a *pe35* ko pRD1-2F9 construct (Fig. 4) was integrated into *M. tuberculosis* H37RvΔRD1, ESAT-6 and CFP-10 proteins were not detected in either whole-cell lysate or the supernatant (*pe35* ko, Fig.5Ba). These results were confirmed independently by the observation that a *pe35* ko mutant of *M. tuberculosis* MT103, isolated by signature-tagged mutagenesis, also lacked CFP-10 and ESAT-6 completely and PPE68 (Fig.5Ba). To investigate whether loss of PE35 acted at the transcriptional level, focused miniarray analysis of gene expression was performed with the appropriate cDNA probes. This revealed that *esxB/A* genes were not transcribed in the PE35 mutant (Fig.5Bc). To evaluate whether the lack of ESAT-6 expression in the *pe35* ko mutants was due to polarity from the transposon insertion, the previously described promoter region [Δprom(*esxB/A*)] (4) or a region even farther upstream located in the 3′ end of gene *ppe68* (Δ*ppe68*) was deleted from pRD1-2F9 (Fig. 4). For the construct that was missing the described promoter region, only trace amounts of ESAT-6 and CFP-10 were found, whereas the recombinant strain lacking the segment further upstream of the described promoter (Δ*ppe68*) did produce large amounts of ESAT-6 and CFP-10 (Fig. 5C). From these experiments we concluded that CFP-10 and ESAT-6 are indeed expressed from their own promoter upstream of *esxB* and should not be subject to downstream effects of the transposon insertion in *pe35*. Together, these findings suggest that PE35 plays a role in the regulation of *esxB/A* expression, a hypothesis, which can now be tackled by more in-depth studies.

Regarding *esxB* (Rv3874), an in-frame deletion of 46 codons resulted in absence of CFP-10 from recombinant BCG (Fig. 5A) or *M. microti*. More surprisingly, in this strain ESAT-6 was not detected either. Three recombinant BCG::RD1 strains with in-frame deletions, lacking the complete *esxA* (Rv3875) gene (Δ*esxA*), or 20 to 22 codons from either end of *esxA* (*esxAΔ3-24* and *esxAΔ76-95*), showed similar phenotypes. Neither ESAT-6 nor CFP-10 were detectable in the cell lysates and supernatants of these strains, suggesting that their expression is tightly linked to each other.

Concerning Rv3876, located downstream of *esxA*, two different recombinants were constructed: an insertion mutant (Rv3876 ko) and an in-frame deletion mutant lacking two-thirds of the gene (ΔRv3876 [Fig. 4]). For both recombinant BCG strains, ESAT-6 and CFP-10 were detected in the culture supernatant, implying that Rv3876 may not be directly involved in the secretion of the two antigens (Fig. 5A). Furthermore, secretion of CFP-10 was reduced when Rv3877 was interrupted (data not shown). The remaining two RD1-associated genes absent from BCG, Rv3878 and Rv3879, are not necessary for the export of the antigens since recombinant strains harboring pRD1-2F9 with the segment from Rv3878 to Rv3881 deleted efficiently secreted the antigens, confirming previous results with a clinical isolate naturally deleted for these genes (Fig. 5A) (35).

Export of whole ESAT-6 is required to elicit ESAT-6-specific T-cell immune responses. To substantiate in vitro secretion results, splenocytes from C57BL/6 mice immunized with various recombinant strains were tested for their capacity to mount ESAT-6- and CFP-10-specific T-cell responses. Inoculation with Rv3868 ko, Rv3869 ko, Rv3870 ko, Rv3871 ko, Δ*esxB*, Δ*esxA*, *esxAΔ3-24*, *esxAΔ76-95*, or *rv3877* ko strains did not induce ESAT-6 specific IFN-γ production by splenocytes (Table 1). In contrast, ΔRv3860-64, ΔRv3860-66, Rv3864 ko, Rv3867 ko, and Rv3876 ko strains elicited ESAT-6-specific IFN-γ responses comparable to those induced by BCG::RD1 and *M. microti*::RD1, emphasizing the accuracy of the in vitro secretion results. In summary, an ESAT-6-specific T-cell response was obtained for the recombinant strains that were not only expressing ESAT-6 and CFP-10 but also secreting the two antigens. As such, the IFN-γ production is a reliable readout system to evaluate whether or not ESAT-6 was secreted by the various recombinant strains.

However, this finding was only true for recombinant strains, which carried a full-length *esxA* gene. Mice infected with BCG::RD1 lacking 12 residues of the extreme C terminus of ESAT-6 (*esxAΔ84-95*) (6) did not develop ESAT-6-specific immune responses in spite of normal secretion of the truncated ESAT-6 molecules (Table 1). It is noteworthy that the T-cell epitope ($CD4^+$), which is located within the N-terminal region of ESAT-6, is not absent in this strain.

Pathogenicity of BCG::RD1 and *M. microti*::RD1 strains correlates with ESAT-6 immunogenicity. Since the SCID mouse model provides a relatively fast screen for virulence, the above-described BCG::RD1 and *M. microti*::RD1 mutants were assayed for their virulence in vivo as outlined previously (8, 34). We tested previously constructed recombinant BCG strains (35) that contained only partial sections of the RD1 region (pAP34, pAP35, and pI106) and do not efficiently secrete ESAT-6 and CFP-10 proteins, and we found no increase in bacterial load relative to the BCG::pYUB412 vector control strain (Table 1).

The same attenuated phenotype was observed for *M. microti* ko strains that were impaired in the export of ESAT-6 due to interruption of a gene whose encoded protein is predicted to be part of the ESX-1 secretion system (e.g., Rv3868, Rv3869, Rv3870, and Rv3871) (Table 1). On the other hand, mice that were infected with recombinant *M. microti* strains inactivated in genes not involved in ESAT-6 secretion (Rv3860-64, Rv3864 ko, Rv3867 ko, *ppe68* ko, ΔRv3876, or Rv3876 ko) showed severe splenomegaly and high bacterial counts in their lungs and spleens similar to those of *M. microti*::RD1 controls. However, one exception was found for *M. microti* ΔRv3860-66 strain, which secreted ESAT-6 and retained antigen-specific T-cell immunogenicity (Fig. 5A and Table 1) without showing enhanced in vivo growth in SCID mice.

As with *M. microti*::RD1 constructs, a correlation between the capacity to induce immune responses to ESAT-6 and CFP-10 and enhanced in vivo growth was obtained for BCG::RD1 strains, which were inactivated for genes in the region of *pe35* to Rv3877. Indeed, insertions or deletions in genes encoding PE35, CFP-10 (EsxB, Rv3874), and ESAT-6 (EsxA, Rv3875) resulted in an attenuated phenotype. Again, disruption of *ppe68* or *rv3876* within recombinant BCG::RD1 strains led to enhanced in vivo growth in SCID mice as seen for *M. microti*. Interestingly, a BCG strain carrying a truncated copy of *ppe68* was even more virulent

TABLE 1. Comparison of ESX-1-specific T-cell immunity and virulence obtained with *M. microti* and BCG recombinants containing modified pRD1-2F9 cosmids[a]

Recombinant strain	Immunogenicity (IFN-γ [ng/ml])			Virulence in SCID mice (ratio of CFU at day 30 relative to that at day 0)		A/V phenotype
	ESAT-6:1-20	rESAT-6	rCFP-10	Lungs	Spleen	
M. microti						
pYUB412	<	<	<	4	2	A, − control
pRD1-2F9	16	20	17	100	80	V, + control
ΔRv3860-64	22	17	16	94	26	V
ΔRv3860-66	12	12	10	14	2	A
Rv3864 ko	10	14	10	19	42	V
Rv3867 ko	19	14	17	2,133	12	V
Rv3868 ko	<	<	<	5	1.3	A
Rv3869 ko	<	<	<	13	2	A
Rv3870 ko	<	<	<	1.2	3.2	A
Rv3871 ko	<	<	<	23	2	A
ppe68 ko	18	12	8	288	16.2	V
Δ*esxB*	<	<	<	ND	ND	A*
Δ*esxA*	<	<	<	ND	ND	A*
*esxA*Δ*3-24*	<	<	<	ND	ND	
Rv3876 ko	<	5	6	39.5	79.6	V
ΔRv3876	<	4	5	644	47	V
Rv3869-79	<	<	<	4	2.9	A
BCG						
pYUB412	<	<	<	15	86	A, − control
pRD1-2F9	22	22	21	15,066	1,095	V, + control
pAP34	<*	<*	<*	3	8	A
pAP35	<*	<*	<*	1	11	A
pI106	<*	<*	<*	34	2	A
ppe68 ko	16	18	14	59,627	210	V
Δ*esxB*	<	<	<	ND	ND	A*
*esxA*Δ*3-24*	<	<	<	ND	ND	
Δ*esxA*	<	<	<	ND	ND	A*
*esxA*Δ*76-95*	<	<	<	ND	ND	
*esxA*Δ*84-95*	<	<	<	17	18	A
Rv3876 ko	18	19	10	6,247	184	V
ΔRv3876	7	9	6	533	180	V
Rv3877 ko	<	<	<	ND	ND	A*
ΔRv3878-81	20	23	22	ND	ND	V*
Rv3869-79	20	19	10	3,840	702	V

[a] The concentration of IFN-γ in the culture supernatants of splenocytes that were stimulated with ESAT-6:1-20 peptide, recombinant ESAT-6 protein (rESAT-6), or recombinant CFP-10 protein (rCFP-10) is given. In all cases, efficient immunization and specificity of IFN-γ secretion by splenocytes was validated with purified protein derivative and MalE:100-114 peptide as positive and negative controls, respectively. The results are from at least two independent experiments with three mice and are expressed as mean values of duplicate culture wells. The standard deviations are within 10%. The "<" symbol indicates that the signal was below the detection limit (1 ng/ml). The ratio of CFU at day 30 relative to the initial dose recovered from the lungs and spleen of SCID mice after intravenous infection with 10^6 CFU is also given. Each value is the mean of three mice. Note that CFU ratios from the lungs after intravenous infection have been observed to be subject to interexperimental variation and should be read relative to the positive and negative controls. A, Attenuated phenotype similar to pYUB412-complemented negative controls; V, virulent phenotype, similar to pRD1-2F9-complemented positive controls. In addition, animals infected with strains classified as "V" showed bad health conditions with respect to the appearance of their fur, their reactiveness, and splenomegaly at the time of sacrifice relative to animals infected with strains classified as "A." An asterisk indicates that an immunogenicity a virulence evaluation in the *M. tuberculosis* complex was reported previously (23, 26, 35, 40). ND, not determined.

than BCG::RD1, since mice died within 3 weeks postinfection, before the end of the experiment (Table 1).

DISCUSSION

The goal of this study was to define the gene set required for production of a functional ESX-1 system by using biologically relevant in vitro and in vivo screens. Unlike bacterial type III or IV secretion processes, ESAT-6 secretion occurs in in vitro grown cultures and does not seem to require host cell target interaction for translocation of the secreted proteins. According to their relevance in this process, the analyzed genes can be grouped into four classes (Table 2).

Inactivation of genes from the first class led to absence of ESAT-6 and CFP-10 from cell lysates of the tested recombinants. Whereas our data confirmed what was previously published for *esxA* and *esxB* (14, 23), to our knowledge this is the first report describing the importance of gene *pe35* (Rv3872) for expression of CFP-10 and ESAT-6. It is encouraging that the two *pe35* ko mutants, which were obtained by independent approaches, both yielded the same results concerning *esxB*/*A* expression, and this result opens new perspectives for studying the regulation of ESX-1 genes.

Interruption or deletion of genes from the second group abolished ESAT-6 export but not its expression. Some of the genes from this group were proposed previously as being involved in secretion of ESAT-6 (Rv3877, Rv3871, and Rv3870) (23, 35, 40), whereas others (Rv3868 and Rv3869) are reported here for the first time in the *M. tuberculosis* complex. The involved genes encode for Rv3868, a chaperone-like protein with an ATP binding site; Rv3869, Rv3870, and Rv3877, three

TABLE 2. Inactivation of the listed genes results in four different phenotypes[a]

Class	Inactivated gene(s)	CFP-10–ESAT-6		ESAT-6-specific immune response	RD1-mediated virulence
		Expression	Secretion		
1	*pe35* (Rv3872), *esxB* (Rv3874), and *esxA* (Rv3875)	No	No	No	No
2	Rv3868, Rv3869, Rv3870, Rv3871, and Rv3877	Yes	No	No	No
3	Rv3864, Rv3867, *ppe68* (Rv3873), Rv3876, and Rv3878/Rv3879	Yes	Yes	Yes	Yes
4	Rv3865/Rv3866	Yes	Yes	Yes	No

[a] *esxB* encodes for CFP-10, and *esxA* encodes for ESAT-6. The expression and secretion of CFP-10 and ESAT-6 are monitored by Western blot analysis of mycobacterial whole-cell extract and culture filtrates. The ESAT-6-specific immune response corresponds to the generation of IFN-γ after in vitro stimulation by ESAT-6 of splenocytes from immunized mice. RD1-mediated virulence is determined by numbering the bacterial load 4 weeks after infection of SCID mice.

putative membrane proteins containing 1-, 3-, or 11-transmembrane domains; and Rv3871 containing an ATP-binding site. The last four proteins may form a membrane-bound complex that is involved in the translocation of ESAT-6 and CFP-10. It is likely that this transport is powered by ATP hydrolysis. For constructs with inactivated genes from class 2, the inability to secrete ESAT-6–CFP-10 resulted in a lack of antigen specific immunogenicity and led to an attenuated phenotype, which is similar to what was observed for genes of class 1. Although the orthologue of Rv3868 was reported to be part of the RD1-encoded locus that regulates DNA transfer in *Mycobacterium smegmatis* (17), in another study Rv3868 was not found to be implicated in the secretion of the *M. smegmatis* ESAT-6 and CFP-10 orthologues (15). In the phylogenetically more closely related *Mycobacterium marinum*, Rv3868 was reported to be involved in the secretion of ESAT-6 and CFP-10 orthologues (21).

In contrast, inactivation of genes from the third class comprising Rv3864, Rv3867, *ppe68* (Rv3873), Rv3876, Rv3878, and Rv3879 did not abolish ESAT-6 secretion, ESAT-6-specific immunogenicity, and enhanced virulence. Truncation or inactivation of PPE68 even led to a moderate increase of secreted ESAT-6, suggesting that this protein could possibly act as a gating protein that regulates the release of ESX-1 antigens. For gene Rv3876, Guinn et al. reported that the gene product is needed for secretion of ESAT-6 (23). We found that an in-frame deletion of more than half of Rv3876 did not affect the secretion and the enhanced in vivo growth phenotype of the complemented BCG strain, suggesting that the results observed by Guinn et al. may have been caused by polar effects of the transposon insertion on gene Rv3877, which is required for secretion.

The fourth group is constituted by Rv3865/Rv3866, whose deletion led to the attenuation of the recombinant strain, in spite of strong ESAT-6 secretion and generation of specific T-cell responses. In a recent study, Rv3865 was found to be abundant in culture medium of a clinical *M. tuberculosis* isolate belonging to the Beijing family (1), and Rv3866 has recently been proposed to be specifically involved in the anaerobic growth of *M. tuberculosis* (41). For *M. smegmatis* and *M. marinum* (15, 21), the Rv3866 orthologues were described as being implicated in the secretion of ESAT-6 and CFP-10 orthologues, whereas in *M. leprae* the Rv3865 orthologue is decayed and Rv3866 is a pseudogene (30). Further studies are needed to clarify the roles of Rv3865 and Rv3866 in *M. tuberculosis*, which may represent a new class of important RD1-associated virulence factors, independent of ESAT-6 secretion or alternatively, possibly involved in stabilizing or modifying the ESAT-6–CFP-10 complex. Although some common traits can be found for ESX-1-related data from various mycobacterial species, it seems that there exist several specific differences for the ESX-1 system in the various mycobacteria, which may reflect the adaptation processes to the requirements of each species. In addition, some proteins encoded elsewhere in the genome may also play a role (20).

As shown in detail in Table 1, one of the main conclusions that can be drawn from the results with the first three classes of mutants are that in general export of ESAT-6 correlates with antigen-specific induction of IFN-γ immune recognition and that RD1-induced virulence requires a functional ESX-1 secretion apparatus. This suggests that ESAT-6 is not processed by the antigen-presenting cells of the mouse, nor does it fulfill its biological role in the infection process if it remains inside the cytosol of the bacterium. The need for an active process probably involving interaction with host cell proteins is further substantiated by the observation that a recombinant BCG strain secreting truncated ESAT-6 (*esxAΔ84-95*) (6) was impaired to induce ESAT-6 specific IFN-γ production in the mouse (Table 1). It seems plausible that the C terminus of ESAT-6 may be involved in such an interaction. These observations are consistent with a major premise of mycobacterial vaccinology, which states that vaccination with BCG only induces efficient protection when live BCG is administered and not if heat-killed cells are used (38), suggesting that active secretion of a wide range of mycobacterial antigens is a prerequisite for generation of a protective immune response.

It was shown that in immunocompetent mice increased virulence of ESX-1 complemented strains may be compensated for by a strong, RD1-encoded antigen-specific activation of cells involved in innate or adaptive immunity (29). In the present study we have substantiated this observation by intravenous infection of mice impaired in IFN-γ or TNF-α signaling pathways, confirming the important role of these cytokines in the normal control of the infection. However, it is still not clear why, in the absence of T-cell-mediated immune responses, RD1-complemented bacteria tend to show enhanced in vivo growth characteristics. The finding that bone-marrow-derived macrophages take up ESAT-6-secreting recombinant strains more efficiently than ESX-1-negative control strains may in part be responsible for this effect. However, further studies involving a set of defined ESX-1 mutant strains are needed to identify the ESX-1 effector molecules and the putative macrophage receptor responsible for this phenomenon.

ACKNOWLEDGMENTS

We thank Mary Jackson and Brigitte Gicquel for helpful discussions; Jean-François Bureau for IFN-γ ko mice; Sabine Maurin, Huot Khun, and Michel Huerre for immunohistochemistry; Elisabeth Couvé for help with macroarrays; Marie-Jésus Rojas for help with immunological experiments; and Eddie Maranghi for expert assistance in animal care.

This study was funded in part by grants from the Institut Pasteur (PTR-110 and GPH-5), the Ministère de la Recherche et Nouvelles Technologies (ACI Microbiologie), the European Community (QLK2-CT-2001-02018 and LSHG-CT-2003-503265), the Association Française Raoul Follereau, and the Wellcome Trust for funding the multi-collaborative microbial pathogen microarray facility under its Functional Genomics Resources Initiative. P.B. recently joined the Institut National de la Santé et de la Recherche Médicale.

REFERENCES

1. **Bahk, Y. Y., S. A. Kim, J. S. Kim, H. J. Euh, G. H. Bai, S. N. Cho, and Y. S. Kim.** 2004. Antigens secreted from *Mycobacterium tuberculosis*: identification by proteomics approach and test for diagnostic marker. Proteomics **4:**3299–3307.
2. **Bange, F. C., F. M. Collins, and W. R. Jacobs, Jr.** 1999. Survival of mice infected with *Mycobacterium* smegmatis containing large DNA fragments from *Mycobacterium tuberculosis*. Tuberc. Lung Dis. **79:**171–180.
3. **Behr, M. A., M. A. Wilson, W. P. Gill, H. Salamon, G. K. Schoolnik, S. Rane, and P. M. Small.** 1999. Comparative genomics of BCG vaccines by whole-genome DNA microarray. Science **284:**1520–1523.
4. **Berthet, F. X., P. B. Rasmussen, I. Rosenkrands, P. Andersen, and B. Gicquel.** 1998. A *Mycobacterium tuberculosis* operon encoding ESAT-6 and a novel low-molecular-mass culture filtrate protein (CFP-10). Microbiology **144:**3195–3203.
5. **Braunstein, M., B. J. Espinosa, J. Chan, J. T. Belisle, and W. R. Jacobs, Jr.** 2003. SecA2 functions in the secretion of superoxide dismutase A and in the virulence of *Mycobacterium tuberculosis*. Mol. Microbiol. **48:**453–464.
6. **Brodin, P., M. I. de Jonge, L. Majlessi, C. Leclerc, M. Nilges, S. T. Cole, and R. Brosch.** 2005. Functional analysis of ESAT-6, the dominant T-cell antigen of *Mycobacterium tuberculosis*, reveals key residues involved in secretion, complex-formation, virulence and immunogenicity. J. Biol. Chem. **80:**33953–33959.
7. **Brodin, P., K. Eiglmeier, M. Marmiesse, A. Billault, T. Garnier, S. Niemann, S. T. Cole, and R. Brosch.** 2002. Bacterial artificial chromosome-based comparative genomic analysis identifies *Mycobacterium microti* as a natural ESAT-6 deletion mutant. Infect. Immun. **70:**5568–5578.
8. **Brodin, P., L. Majlessi, R. Brosch, D. Smith, G. Bancroft, S. Clark, A. Williams, C. Leclerc, and S. T. Cole.** 2004. Enhanced protection against tuberculosis by vaccination with recombinant *Mycobacterium microti* vaccine that induces T-cell immunity against region of difference 1 antigens. J. Infect. Dis. **190:**115–122.
9. **Brodin, P., I. Rosenkrands, P. Andersen, S. T. Cole, and R. Brosch.** 2004. ESAT-6 proteins: protective antigens and virulence factors? Trends Microbiol. **12:**500–508.
10. **Bronstein, P., M. Marrichi, and M. P. DeLisa.** 2004. Dissecting the twin-arginine translocation pathway using genome-wide analysis. Res. Microbiol. **155:**803–810.
11. **Brosch, R., S. V. Gordon, A. Billault, T. Garnier, K. Eiglmeier, C. Soravito, B. G. Barrell, and S. T. Cole.** 1998. Use of a *Mycobacterium tuberculosis* H37Rv bacterial artificial chromosome library for genome mapping, sequencing, and comparative genomics. Infect. Immun. **66:**2221–2229.
12. **Brosch, R., S. V. Gordon, M. Marmiesse, P. Brodin, C. Buchrieser, K. Eiglmeier, T. Garnier, C. Gutierrez, G. Hewinson, K. Kremer, L. M. Parsons, A. S. Pym, S. Samper, D. van Soolingen, and S. T. Cole.** 2002. A new evolutionary scenario for the *Mycobacterium tuberculosis* complex. Proc. Natl. Acad. Sci. USA **99:**3684–3689.
13. **Cole, S. T., R. Brosch, J. Parkhill, T. Garnier, C. Churcher, D. Harris, S. V. Gordon, K. Eiglmeier, S. Gas, C. E. Barry III, F. Tekaia, K. Badcock, D. Basham, D. Brown, T. Chillingworth, R. Connor, R. Davies, K. Devlin, T. Feltwell, S. Gentles, N. Hamlin, S. Holroyd, T. Hornsby, K. Jagels, B. G. Barrell, et al.** 1998. Deciphering the biology of *Mycobacterium tuberculosis* from the complete genome sequence. Nature **393:**537–544.
14. **Collins, D. M., B. Skou, S. White, S. Bassett, L. Collins, R. For, K. Hurr, G. Hotter, and G. W. de Lisle.** 2005. Generation of attenuated *Mycobacterium bovis* strains by signature-tagged mutagenesis for discovery of novel vaccine candidates. Infect. Immun. **73:**2379–2386.
15. **Converse, S. E., and J. S. Cox.** 2005. A protein secretion pathway critical for *Mycobacterium tuberculosis* virulence is conserved and functional in *Mycobacterium* smegmatis. J. Bacteriol. **187:**1238–1245.
16. **Demangel, C., P. Brodin, P. J. Cockle, R. Brosch, L. Majlessi, C. Leclerc, and S. T. Cole.** 2004. Cell envelope protein PPE68 contributes to *Mycobacterium tuberculosis* RD1 immunogenicity independently of a 10-kilodalton culture filtrate protein and ESAT-6. Infect. Immun. **72:**2170–2176.
17. **Flint, J. L., J. C. Kowalski, P. K. Karnati, and K. M. Derbyshire.** 2004. The RD1 virulence locus of *Mycobacterium tuberculosis* regulates DNA transfer in *Mycobacterium smegmatis*. Proc. Natl. Acad. Sci. USA **101:**12598–12603.
18. **Flynn, J. L., J. Chan, K. J. Triebold, D. K. Dalton, T. A. Stewart, and B. R. Bloom.** 1993. An essential role for interferon gamma in resistance to *Mycobacterium tuberculosis* infection. J. Exp. Med. **178:**2249–2254.
19. **Flynn, J. L., M. M. Goldstein, J. Chan, K. J. Triebold, K. Pfeffer, C. J. Lowenstein, R. Schreiber, T. W. Mak, and B. R. Bloom.** 1995. Tumor necrosis factor-alpha is required in the protective immune response against *Mycobacterium tuberculosis* in mice. Immunity **2:**561–572.
20. **Fortune, S. M., A. Jaeger, D. A. Sarracino, M. R. Chase, C. M. Sassetti, D. R. Sherman, B. R. Bloom, and E. J. Rubin.** 2005. Mutually dependent secretion of proteins required for mycobacterial virulence. Proc. Natl. Acad. Sci. USA **102:**10676–10681.
21. **Gao, L. Y., S. Guo, B. McLaughlin, H. Morisaki, J. N. Engel, and E. J. Brown.** 2004. A mycobacterial virulence gene cluster extending RD1 is required for cytolysis, bacterial spreading, and ESAT-6 secretion. Mol. Microbiol. **53:**1677–1693.
22. **Gordon, S. V., R. Brosch, A. Billault, T. Garnier, K. Eiglmeier, and S. T. Cole.** 1999. Identification of variable regions in the genomes of tubercle bacilli using bacterial artificial chromosome arrays. Mol. Microbiol. **32:**643–655.
23. **Guinn, K. M., M. J. Hickey, S. K. Mathur, K. L. Zakel, J. E. Grotzke, D. M. Lewinsohn, S. Smith, and D. R. Sherman.** 2004. Individual RD1-region genes are required for export of ESAT-6/CFP-10 and for virulence of *Mycobacterium tuberculosis*. Mol. Microbiol. **51:**359–370.
24. **Hsu, T., S. M. Hingley-Wilson, B. Chen, M. Chen, A. Z. Dai, P. M. Morin, C. B. Marks, J. Padiyar, C. Goulding, M. Gingery, D. Eisenberg, R. G. Russell, S. C. Derrick, F. M. Collins, S. L. Morris, C. H. King, and W. R. Jacobs, Jr.** 2003. The primary mechanism of attenuation of bacillus Calmette-Guerin is a loss of secreted lytic function required for invasion of lung interstitial tissue. Proc. Natl. Acad. Sci. USA **100:**12420–12425.
25. **Huang, S., W. Hendriks, A. Althage, S. Hemmi, H. Bluethmann, R. Kamijo, J. Vilcek, R. M. Zinkernagel, and M. Aguet.** 1993. Immune response in mice that lack the interferon-gamma receptor. Science **259:**1742–1745.
26. **Inwald, J., K. Jahans, R. G. Hewinson, and S. V. Gordon.** Inactivation of the *Mycobacterium bovis* homologue of the polymorphic RD1 gene Rv3879c (Mb3909c) does not affect virulence. Tuberculosis **83:**387–393.
27. **Lewis, K. N., R. Liao, K. M. Guinn, M. J. Hickey, S. Smith, M. A. Behr, and D. R. Sherman.** 2003. Deletion of RD1 from *Mycobacterium tuberculosis* mimics Bacille Calmette-Guerin attenuation. J. Infect. Dis. **187:**117–123.
28. **Mahairas, G. G., P. J. Sabo, M. J. Hickey, D. C. Singh, and C. K. Stover.** 1996. Molecular analysis of genetic differences between *Mycobacterium bovis* BCG and virulent *M. bovis*. J. Bacteriol. **178:**1274–1282.
29. **Majlessi, L., P. Brodin, R. Brosch, M. J. Rojas, H. Khun, M. Huerre, S. T. Cole, and C. Leclerc.** 2005. Influence of ESAT-6 secretion system 1 (RD1) of *Mycobacterium tuberculosis* on the interaction between mycobacteria and the host immune system. J. Immunol. **174:**3570–3579.
30. **Marmiesse, M., P. Brodin, C. Buchrieser, C. Gutierrez, N. Simoes, V. Vincent, P. Glaser, S. T. Cole, and R. Brosch.** 2004. Macro-array and bioinformatic analyses reveal mycobacterial "core" genes, variation in the ESAT-6 gene family and new phylogenetic markers for the *Mycobacterium tuberculosis* complex. Microbiology **150:**483–496.
31. **Mostowy, S., D. Cousins, and M. A. Behr.** 2004. Genomic interrogation of the Dassie bacillus reveals it as a unique RD1 mutant within the *Mycobacterium tuberculosis* complex. J. Bacteriol. **186:**104–109.
32. **Okkels, L. M., E. C. Muller, M. Schmid, I. Rosenkrands, S. H. Kaufmann, P. Andersen, and P. R. Jungblut.** 2004. CFP10 discriminates between nonacetylated and acetylated ESAT-6 of *Mycobacterium tuberculosis* by differential interaction. Proteomics **4:**2954–2960.
33. **Pugsley, A. P.** 1993. The complete general secretory pathway in gram-negative bacteria. Microbiol. Rev. **57:**50–108.
34. **Pym, A. S., P. Brodin, R. Brosch, M. Huerre, and S. T. Cole.** 2002. Loss of RD1 contributed to the attenuation of the live tuberculosis vaccines *Mycobacterium bovis* BCG and *Mycobacterium microti*. Mol. Microbiol. **46:**709–717.
35. **Pym, A. S., P. Brodin, L. Majlessi, R. Brosch, C. Demangel, A. Williams, K. E. Griffiths, G. Marchal, C. Leclerc, and S. T. Cole.** 2003. Recombinant BCG exporting ESAT-6 confers enhanced protection against tuberculosis. Nat. Med. **9:**533–539.
36. **Rengarajan, J., B. R. Bloom, and E. J. Rubin.** 2005. Genome-wide requirements for *Mycobacterium tuberculosis* adaptation and survival in macrophages. Proc. Natl. Acad. Sci. USA **102:**8327–8332.
37. **Renshaw, P. S., K. L. Lightbody, V. Veverka, F. W. Muskett, G. Kelly, T. A. Frenkiel, S. V. Gordon, R. G. Hewinson, B. Burke, J. Norman, R. A. Williamson, and M. D. Carr.** 2005. Structure and function of the complex formed by the tuberculosis virulence factors CFP-10 and ESAT-6. EMBO J. **24:**2491–2498.
38. **Romain, F., A. Laqueyrerie, P. Militzer, P. Pescher, P. Chavarot, M. Lagranderie, G. Auregan, M. Gheorghiu, and G. Marchal.** 1993. Identification of a *Mycobacterium bovis* BCG 45/47-kilodalton antigen complex, an immunodominant target for antibody response after immunization with living bacteria. Infect. Immun. **61:**742–750.

39. **Sorensen, A. L., S. Nagai, G. Houen, P. Andersen, and A. B. Andersen.** 1995. Purification and characterization of a low-molecular-mass T-cell antigen secreted by *Mycobacterium tuberculosis*. Infect. Immun. **63:**1710–1717.
40. **Stanley, S. A., S. Raghavan, W. W. Hwang, and J. S. Cox.** 2003. Acute infection and macrophage subversion by *Mycobacterium tuberculosis* require a specialized secretion system. Proc. Natl. Acad. Sci. USA **100:**13001–13006.
41. **Starck, J., G. Kallenius, B. I. Marklund, D. I. Andersson, and T. Akerlund.** 2004. Comparative proteome analysis of *Mycobacterium tuberculosis* grown under aerobic and anaerobic conditions. Microbiology **150:**3821–3829.
42. **Stewart, G. R., L. Wernisch, R. Stabler, J. A. Mangan, J. Hinds, K. G. Laing, D. B. Young, and P. D. Butcher.** 2002. Dissection of the heat-shock response in *Mycobacterium tuberculosis* using mutants and microarrays. Microbiology **148:**3129–3138.
43. **Tekaia, F., S. V. Gordon, T. Garnier, R. Brosch, B. G. Barrell, and S. T. Cole.** 1999. Analysis of the proteome of *Mycobacterium tuberculosis* in silico. Tuberc. Lung Dis. **79:**329–342.
44. **Wiker, H. G., and M. Harboe.** 1992. The antigen 85 complex: a major secretion product of *Mycobacterium tuberculosis*. Microbiol. Rev. **56:**648–661.

Editor: J. L. Flynn